Hindawi Publishing Corporation
Mathematical Problems in Engineering
Volume 2010, Article ID 895785, 15 pages
doi:10.1155/2010/895785

Research Article

Analysis of Large-Amplitude Pulses in Short Time Intervals: Application to Neuron Interactions

Gianni Mattioli,[1] Massimo Scalia,[1] and Carlo Cattani[2]

[1] *Department of Mathematics, "G. Castelnuovo", University of Rome, "La Sapienza", Piazzale Aldo Moro 2, 00185 Rome, Italy*
[2] *DiFarma, University of Salerno, Via Ponte Don Melillo, 84084 Fisciano, Italy*

Correspondence should be addressed to Massimo Scalia, massimo.scalia@uniroma1.it

Received 29 January 2010; Accepted 24 March 2010

Academic Editor: Ming Li

This paper deals with the analysis of a nonlinear dynamical system which characterizes the axons interaction and is based on a generalization of FitzHugh-Nagumo system. The parametric domain of stability is investigated for both the linear and third-order approximation. A further generalization is studied in presence of high-amplitude (time-dependent) pulse. The corresponding numerical solution for some given values of parameters are analyzed through the wavelet coefficients, showing both the sensitivity to local jumps and some unexpected inertia of neuron's as response to the high-amplitude spike.

1. Introduction

The classical model of one excitatory neuron [1–11] is considered under a spike train (time-dependent) excitation. The dynamical system as well as its evolution are investigated under the dependence on some featuring parameters and in presence of a high-amplitude time-dependent pulse. It was already shown, in a previous paper [12], dealing with Hodgkin-Huxley model, that neuron's multiple firing does not reflects immediately on a direct response and there is some kind of time delay (inertia) before the pulse becomes effective. It should be noticed that there are different models of neurons (see, e.g., [1] and references therein) such as the Integrate-and-fire, FitzHugh-Nagumo [2, 9], Morris-Lecar, and the more general Hodgkin-Huxley model [6–8]. In the early sixties, FitzHugh [2] proposed, as a simplified model, a generalization of the Van der Pol equation thus showing the existence of a limit cycle and some periodicity. In all models, if we consider a simple system consisting of a neuron and a synapse, it is known that the activity of stimulated axons can be detected by an abrupt change in the electrical potential. These pulse in a short time are called spikes or axons firing. However, as shown later these abrupt changes do not appear immediately, thus

showing, even in this simplified model of neurons interactions, the existence of some kind of neurons inertia, which can be physically explained by their cooperative responce to firing.

In the following we will propose a suitable generalization of the FitzHugh-Nagumo model (FHN) and we will study both on the linear and third-order approximation. Equilibrium points, parametric domain of stability will be outlined in absence of time-dependence. The presence of high-amplitude time-dependent source of pulses can be studied on the nonlinear time series of the numerical approximation. The pulse action of the firing process, based on FitzHugh suggestion of delta Dirac function, is proposed in the form of a high-amplitude localized function with compact support in a short interval, which replicates a few times before it disappears. According to FitzHugh any change in the electrical potential are localized in a short time interval and within this interval has a significant amplitude.

2. Simplified FitzHugh-Nagumo Model

The most successful and general model in neuroscience describes the neuron activity in terms of two conductances and electric potentials. The Hodgkin-Huxley model [6–8] considers the neuron activity as an electrical circuit. Cells membrane store charges, electrochemical forces arise because of the imbalanced ion concentration inside and outside the cell. It can be written, in adimensional form, as

$$\begin{aligned}
\frac{du}{dt} &= a_1 n^4 (a_2 - u) + a_3 m^3 h (a_4 - u) + a_5 (a_6 - u) - I_{\text{ext}}(t), \\
\frac{dn}{dt} &= \alpha_n(u)(1 - n) - \beta_n(u) n, \\
\frac{dm}{dt} &= \alpha_m(u)(1 - m) - \beta_m(u) m, \\
\frac{dh}{dt} &= \alpha_h(u)(1 - h) - \beta_h(u) h,
\end{aligned} \tag{2.1}$$

being

$$\begin{aligned}
\alpha_n(u) &= \phi \cdot \frac{a_7(u - a_8)}{1 - e^{-(u-a_8)/a_9}}, \qquad \beta_n(u) = \phi \cdot a_{10} e^{-(u-a_{11})/a_{12}}, \\
\alpha_m(u) &= \phi \cdot \frac{a_{13}(u - a_{14})}{1 - e^{-(u-a_{14})/a_{15}}}, \qquad \beta_m(u) = \phi \cdot a_{16} e^{-(u-a_{17})/a_{18}}, \\
\alpha_h(u) &= \phi \cdot a_{19} e^{-(u-a_{20})/a_{21}}, \qquad \beta_h(u) = \phi \cdot \frac{a_{22}}{1 + e^{-(u-a_{23})/a_{24}}}.
\end{aligned} \tag{2.2}$$

An alternative simplified 2-dimensional model (FHN) that has been proposed by FitzHugh-Nagumo [2, 9] can be substantially represented by the system

$$\begin{aligned}
\frac{dx}{dt} &= a\left(x - \frac{x^3}{3}\right) - by + \gamma z, \\
\frac{dy}{dt} &= \alpha x - \beta y,
\end{aligned} \tag{2.3}$$

where $z = z(t)$ is a pulse function defined in a very short-range interval (pulse function), having as limiting case the delta Dirac. In the following we will consider a spike train. Parameter γ defines the amplitude of the pulse function $z(t)$.

This dynamical system depends [2, 9] on a, b, α, β, and γ in the sense that the evolution would be completely different, starting from some critical values. In the following we will show that the solution tends asymptotically to a constant value.

A suitable generalization of system (2.3) is

$$\begin{aligned} \frac{dx}{dt} &= a\sin x - bh(y) + \gamma z(t), \\ \frac{dy}{dt} &= \alpha f(x) - \beta g(y), \end{aligned} \tag{2.4}$$

with nonnegative parameters

$$a \geq 0, \qquad b \geq 0, \qquad \beta \geq 0, \tag{2.5}$$

and odd functions

$$\begin{aligned} f(x) = -f(-x), \qquad h(y) = h(-y), \qquad g(y) = g(-y), \\ f(x_0) = f''(x_0) = f''''(x_0) = 0, \\ h(x_0) = h''(x_0) = h''''(x_0) = 0, \\ g(x_0) = g''(x_0) = g''''(x_0) = 0. \end{aligned} \tag{2.6}$$

Up to the first-order it is

$$\begin{aligned} \frac{dx}{dt} &= ax - by + \gamma z(t), \\ \frac{dy}{dt} &= \alpha x - \beta y, \end{aligned} \tag{2.7}$$

and to the third-order it is

$$\begin{aligned} \frac{dx}{dt} &= a\left(x - \frac{x^3}{6}\right) - by + \gamma z(t), \\ \frac{dy}{dt} &= \alpha x - \beta y, \end{aligned} \tag{2.8}$$

so that the FHN system (2.3) might be considered as the third-order approximation of system (2.4).

2.1. Autonomous System $\gamma = 0$

2.1.1. Linear Case

When $\gamma = 0$, and assuming by analogy with system (2.3) that

$$a = 1, \qquad b = 1, \tag{2.9}$$

from the linear system (2.7), we have

$$\frac{dx}{dt} = x - y, \tag{2.10a}$$

$$\frac{dy}{dt} = \alpha x - \beta y. \tag{2.10b}$$

There is only one equilibrium point at the origin:

$$(\overline{x}, \overline{y}) = (0, 0). \tag{2.11}$$

The eigenvalues are

$$\lambda_{1,2} = \frac{1}{2}\left(1 - \beta \pm \sqrt{\Delta}\right), \qquad \Delta \equiv 1 - 4\alpha + 2\beta + \beta^2. \tag{2.12}$$

The parametric domain of feasible values for α and β is defined according to (2.5) and by the parabolic curve as in Figure 1:

$$\alpha = \frac{1}{4}(\beta + 1)^2. \tag{2.13}$$

Thus we have

$$\lambda_1 = \lambda_2 \in \mathbb{R}, \qquad \alpha = \frac{\beta^2}{4} + \frac{\beta}{2} + 1, \tag{2.14}$$

where $\beta > 1$, stable equilibrium in $(0, 0)$, and $\beta < 1$, unstable equilibrium in $(0, 0)$;

$$\lambda_1 \neq \lambda_2 \in \mathbb{R}, \qquad \alpha > \frac{\beta^2}{4} + \frac{\beta}{2} + 1, \tag{2.15}$$

where $\lambda_1 < 0$, $\lambda_2 < 0$, stable equilibrium in $(0, 0)$, $\lambda_1 < 0$, $\lambda_2 > 0$, unstable equilibrium in $(0, 0)$ (saddle), and $\lambda_1 > 0$, $\lambda_2 > 0$, unstable equilibrium in $(0, 0)$;

$$\lambda_1 = \lambda_2 \in \mathbb{C}, \qquad \alpha < \frac{\beta^2}{4} + \frac{\beta}{2} + 1, \tag{2.16}$$

where $\beta > 1$, stable equilibrium in $(0, 0)$, and $\beta < 1$, unstable equilibrium in $(0,\ 0)$.

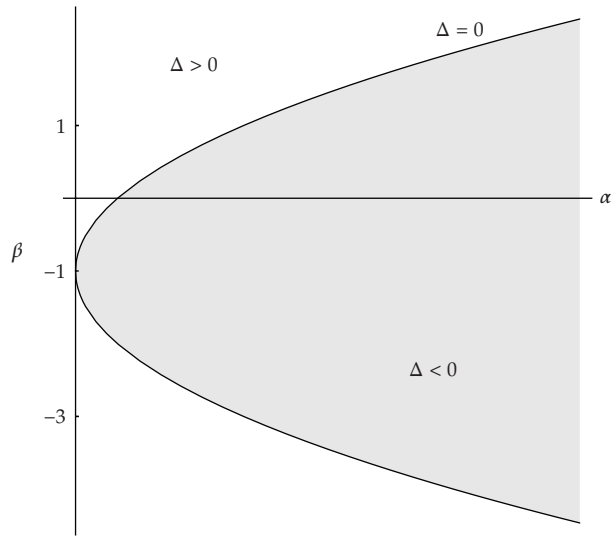

Figure 1: Parametric domain for the linear FHN model (8).

As a special case, by assuming that $t_0 = 0,\ x(0) = x_0,$ and $y(0) = y_0$ with $\alpha = 0, \beta \neq 0$, from (2.10b) we have

$$y(t) = y_0 e^{-\beta t}, \tag{2.17}$$

and from (2.10a) we have

$$x(t) = \begin{cases} x_0 e^t + \dfrac{y_0}{1+\beta}\left[e^{-\beta t} - e^t\right], & \beta \neq -1, \\ e^t(x_0 - y_0 t), & \beta = -1. \end{cases} \tag{2.18}$$

Analogously, by assuming that $t_0 = 0,\ x(0) = x_0,$ and $y(0) = y_0$ with $\beta = 0, \alpha \neq 0$, from (2.10b) we have $(\alpha \neq 1/4)$

$$\begin{aligned} x(t) &= \frac{e^{t/2}}{\sqrt{1-4\alpha}}\left[x_0\sqrt{1-4\alpha}\cosh\left(\frac{\sqrt{1-4\alpha}}{2}t\right) + (x_0 - 2y_0)\sinh\left(\frac{\sqrt{1-4\alpha}}{2}t\right)\right], \\ y(t) &= \frac{e^{t/2}}{\sqrt{1-4\alpha}}\left[y_0\sqrt{1-4\alpha}\cosh\left(\frac{\sqrt{1-4\alpha}}{2}t\right) + (2\alpha x_0 - y_0)\sinh\left(\frac{\sqrt{1-4\alpha}}{2}t\right)\right], \\ x(t) &= \frac{e^{t/2}}{2}\left[x_0(2+t) - 2y_0 t\right], \\ y(t) &= \frac{e^{t/2}}{4}\left[x_0 t - 2y_0(t-2)\right], \end{aligned} \tag{2.19}$$

when $\alpha = 1/4$.

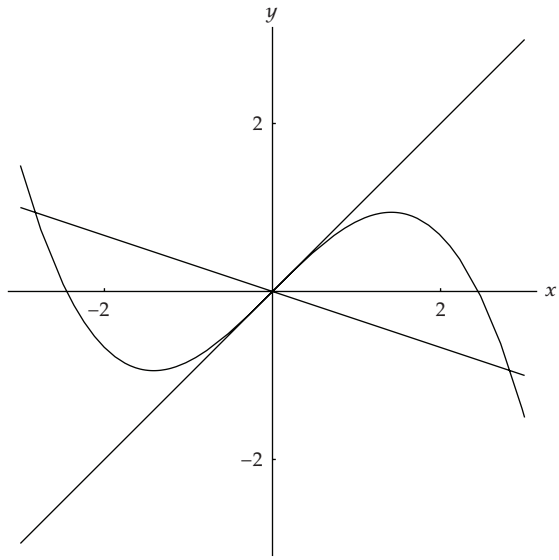

Figure 2: Null clines for (2.21).

2.1.2. Third-Order Approximation

Assuming that

$$a = 1, \qquad b = 1, \tag{2.20}$$

from the third-order system (2.8), we have

$$\begin{aligned} \frac{dx}{dt} &= \left(x - \frac{x^3}{6} \right) - y, \\ \frac{dy}{dt} &= \alpha x - \beta y. \end{aligned} \tag{2.21}$$

The null clines intersect at the points

$$\begin{aligned} (\overline{x}_1, \overline{y}_1) &= (0, 0), \\ (\overline{x}_2, \overline{y}_2) &= \left(-\sqrt{\frac{6(\beta - \alpha)}{\beta}}, -\frac{\alpha}{\beta}\sqrt{\frac{6(\beta - \alpha)}{\beta}} \right), \\ (\overline{x}_3, \overline{y}_3) &= \left(\sqrt{\frac{6(\beta - \alpha)}{\beta}}, \frac{\alpha}{\beta}\sqrt{\frac{6(\beta - \alpha)}{\beta}} \right), \end{aligned} \tag{2.22}$$

so that, being $\beta > 0$, there are 3 disjoint equilibrium points (Figure 2) when

$$\beta > \alpha, \tag{2.23}$$

and only one when

$$\alpha \leq -\beta. \tag{2.24}$$

The Jacobian of (2.21) is

$$J(x,y) = \begin{pmatrix} 1 - \dfrac{x^2}{2} & -1 \\ \alpha & -\beta \end{pmatrix} \tag{2.25}$$

so that

$$J(\overline{x}_2, \overline{y}_2) = J(\overline{x}_3, \overline{y}_3) = \begin{pmatrix} \dfrac{1}{\beta}(3\alpha - 2\beta) & -1 \\ \alpha & -\beta \end{pmatrix}. \tag{2.26}$$

The eigenvalues are

$$\lambda_{1,2} = \frac{1}{2\beta}\left(3\alpha - 2\beta - \beta^2 \pm \sqrt{\Delta_1}\right), \qquad \Delta_1 \equiv (3\alpha - 2\beta)^2 + \beta^2\left(\beta^2 - 4\beta + 2\alpha\right). \tag{2.27}$$

The parametric domain of feasible values for α and β is defined by the curve

$$(3\alpha - 2\beta)^2 + \beta^2\left(\beta^2 - 4\beta + 2\alpha\right) = 0 \tag{2.28}$$

as in Figure 3.

2.1.3. The General Case (2.4)

When $\gamma = 0$, assuming that

$$a = 1, \qquad b = 1, \qquad f(x) = x, \qquad g(y) = y \tag{2.29}$$

from the system (2.4), we have

$$\begin{aligned} \frac{dx}{dt} &= \sin x - y, \\ \frac{dy}{dt} &= \alpha x - \beta y. \end{aligned} \tag{2.30}$$

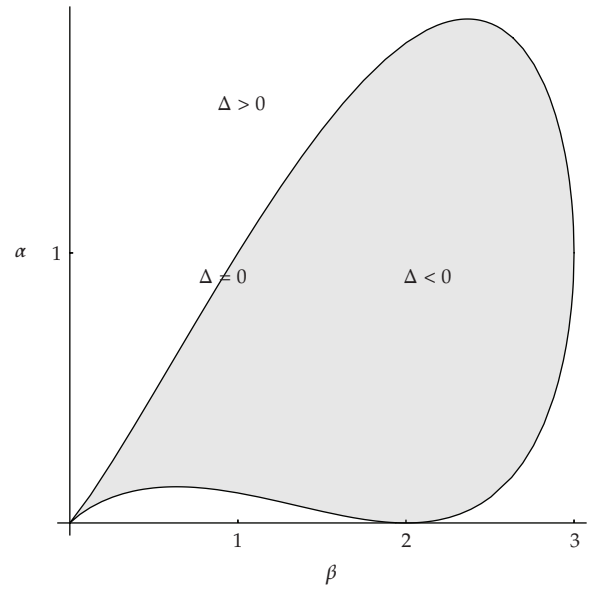

Figure 3: Parametric domain of (2.21).

The null clines have at least two intersections (Figure 4) when

$$\alpha \leq \beta \quad \text{or} \quad \beta \geq -4.6\alpha \tag{2.31}$$

and only one when

$$\alpha \leq \beta. \tag{2.32}$$

otherwise, there are more than one intersection.

The Jacobian of (2.30) and eigenvalues coincide with the linear case.

3. FHN Model with a High-Amplitude Spike

Let us consider the general nonautonomous system (2.4) when $\gamma \neq 0$:

$$\begin{aligned} \frac{dx}{dt} &= \sin x - y + \gamma z(t), \\ \frac{dy}{dt} &= \alpha x - \beta y. \end{aligned} \tag{3.1}$$

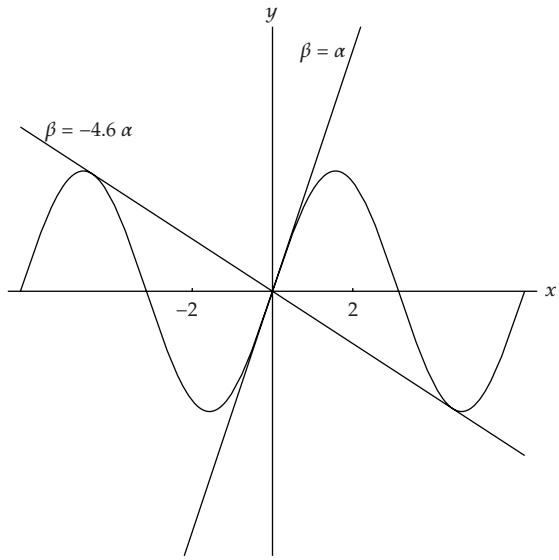

Figure 4: Null clines for (2.8).

The time-dependent function $z(t)$ is a high-amplitude function (Figure 5), based on Haar wavelets

$$z(t) \equiv \sum_{k=-3}^{3} 10\psi_8^4(t-k) + 5\psi_9^4(t-k) + \psi_1^4 0(t-k) \tag{3.2}$$

which replicates itself in a finite interval (Figure 6).

The basic wavelet function $\psi_k^n(t)$ is defined as

$$\psi_k^n(t) \equiv 2^{n/2} \begin{cases} 1, & \dfrac{k}{2^n} \le t < \dfrac{k+0.5}{2^n}, \\ -1, & \dfrac{k+0.5}{2^n} \le t < \dfrac{k+1}{2^n}, \\ 0, & \text{elsewhere.} \end{cases} \tag{3.3}$$

3.1. Numerical Simulation

Let us assume for the values of parameters the following: $\gamma = 10^2$, $\beta = 2$ and two different values for α, that is, $\alpha = -0.01$, $\alpha = 2$ in the interval $t \in [0, 8]$. As initial conditions it is assumed that $x(0) = 0$, $y(0) = 0$. By using the Runge-Kutta 4th-order method, with the accuracy 10^{-6}, we obtain in the interval $(0 < t \le 8)$, the solution in correspondence with different initial conditions.

From a direct inspection of the solution (see Figures 7 and 8) it can be seen that under a spike firing there is some delay effect so that the perturbation show its influence only after some time delay. This perturbation of the system makes the orbits nearby the origin unstable. The uniqueness in phase space is going to be lost at least in the initial time interval. The orbit in the phase plane is self-crossing. The uniqueness of motion is lost. When $\alpha = -0.01$, the origin behaves as an attractor, while in the case $\alpha = 2$, x, y diverge asymptotically.

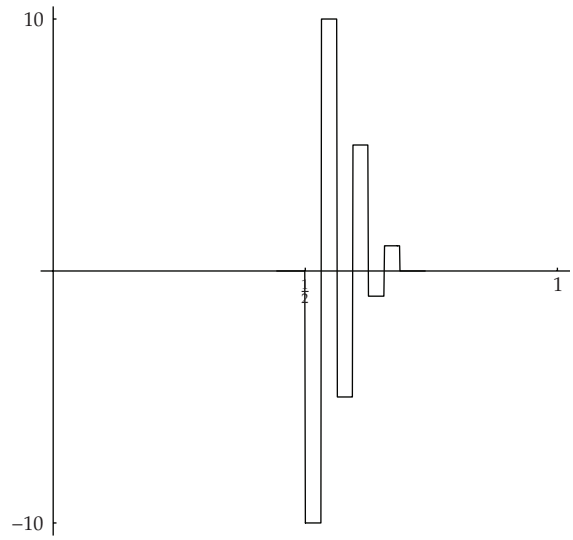

Figure 5: High-amplitude function $10\psi_8^4(t) + 5\psi_9^4(t) + \psi_{10}^4(t)$.

4. Wavelet Analysis

The *Haar scaling function* $\varphi(t)$ is the characteristic function on $[0,1]$. By translation and dilation we get the family of functions defined (in $[0,1]$) as

$$\begin{aligned} \varphi_k^n(t) &\equiv 2^{n/2}\varphi(2^n t - k), \quad (0 \le n,\ 0 \le k \le 2^n - 1), \\ \varphi(2^n t - k) &= \begin{cases} 1, & t \in \Omega_k^n, \\ 0, & t \notin \Omega_k^n, \end{cases} \quad \Omega_k^n \equiv \left[\frac{k}{2^n}, \frac{k+1}{2^n}\right). \end{aligned} \tag{4.1}$$

The *Haar wavelet* family $\{\psi_k^n(t)\}$ is the orthonormal basis [13]:

$$\begin{aligned} \psi_k^n(t) &\equiv 2^{n/2}\psi(2^n t - k), \quad \left\|\psi_k^n(t)\right\|_{L^2} = 1, \\ \psi(2^n t - k) &\equiv \begin{cases} -1, & t \in \left[\dfrac{k}{2^n}, \dfrac{k+1/2}{2^n}\right), \\ 1, & t \in \left[\dfrac{k+1/2}{2^n}, \dfrac{k+1}{2^n}\right), \quad (0 \le n,\ 0 \le k \le 2^n - 1), \\ 0, & \text{elsewhere.} \end{cases} \end{aligned} \tag{4.2}$$

Without loss of generality, we can restrict ourselves to $0 \le n$, $0 \le k \le 2^n - 1 \Rightarrow \Omega_k^n \subseteq [0,1]$. Let $\mathbf{Y} \equiv \{Y_i\}$, $(i = 0, \ldots, 2^M - 1,\ 2^M = N < \infty,\ M \in \mathbb{N})$, be a finite energy time-series; $t_i = i/(2^M - 1)$, is the regular equispaced grid of *dyadic points*.

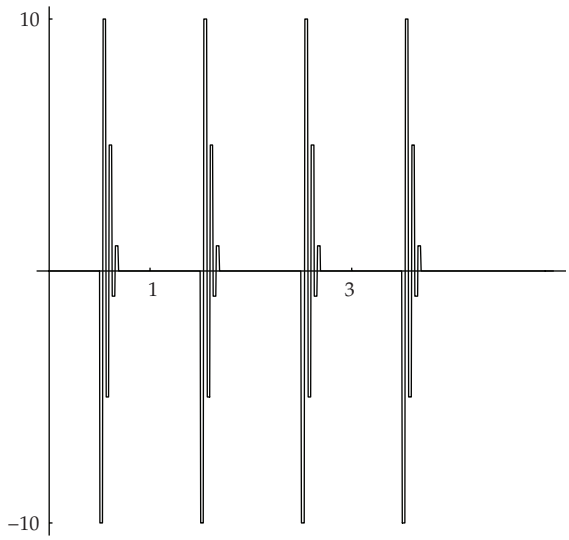

Figure 6: $z(t)$.

The *discrete Haar wavelet transform* is the operator $\mathcal{W}^N$ which maps the vector $\mathbf{Y}$ into the vector of the *wavelet coefficients* $\{\alpha, \beta_k^n\}$:

$$\mathcal{W}^N \mathbf{Y} = \left\{\alpha, \beta_0^0, \ldots, \beta_{2^{M-1}-1}^{M-1}\right\}, \quad \mathbf{Y} = \{Y_0, Y_1, \ldots, Y_{N-1}\}, \tag{4.3}$$

However in order to reduce the computational complexity it has been proposed [14] the short wavelet transform as follows. Let the set $\mathbf{Y} = \{Y_i\}$ of N data be segmented into σ segments (in general) of different length. Each segment $\mathbf{Y}^s$, $s = 0, \ldots, \sigma-1$ is made of $p_s = 2^{m_s}$, $(\sum_s p_s = N)$, data:

$$\mathbf{Y} = \{Y_i\}_{i=0,\ldots,N-1} = \bigoplus_{s=0}^{\sigma-1} \{\mathbf{Y}^s\}, \quad \mathbf{Y}^s \equiv \left\{Y_{sp_s}, Y_{sp_s+1}, \ldots, Y_{sp_s+p_s-1}\right\}, \tag{4.4}$$

being, in general, $p_s \neq p_r$. The short discrete Haar wavelet transform of $\mathbf{Y}$ is (see [14]) $\mathcal{W}^{p_s,\sigma}\mathbf{Y}$,

$$\begin{gathered}
\mathcal{W}^{p_s,\sigma} \equiv \bigoplus_{s=0}^{\sigma-1} \mathcal{W}_s^p, \qquad \mathbf{Y} = \bigoplus_{s=0}^{\sigma-1} \mathbf{Y}^s, \\
\mathcal{W}^{p_s,\sigma}\mathbf{Y} = \left(\bigoplus_{s=0}^{\sigma-1} \mathcal{W}^{p_s}\right)\mathbf{Y} = \left(\bigoplus_{s=0}^{\sigma-1} \mathcal{W}^{p_s}\mathbf{Y}^s\right), \\
\mathcal{W}^{2^{m_s}}\mathbf{Y}^s = \left\{\alpha_0^{0(s)}, \beta_0^{0(s)}, \beta_0^{1(s)}, \beta_1^{1(s)}, \ldots, \beta_{2^{m_s-1}-1}^{m_s-1(s)}\right\},
\end{gathered} \tag{4.5}$$

with $2^{m_s} = p_s$, $\sum_{s=0}^{\sigma-1} p_s = N$.

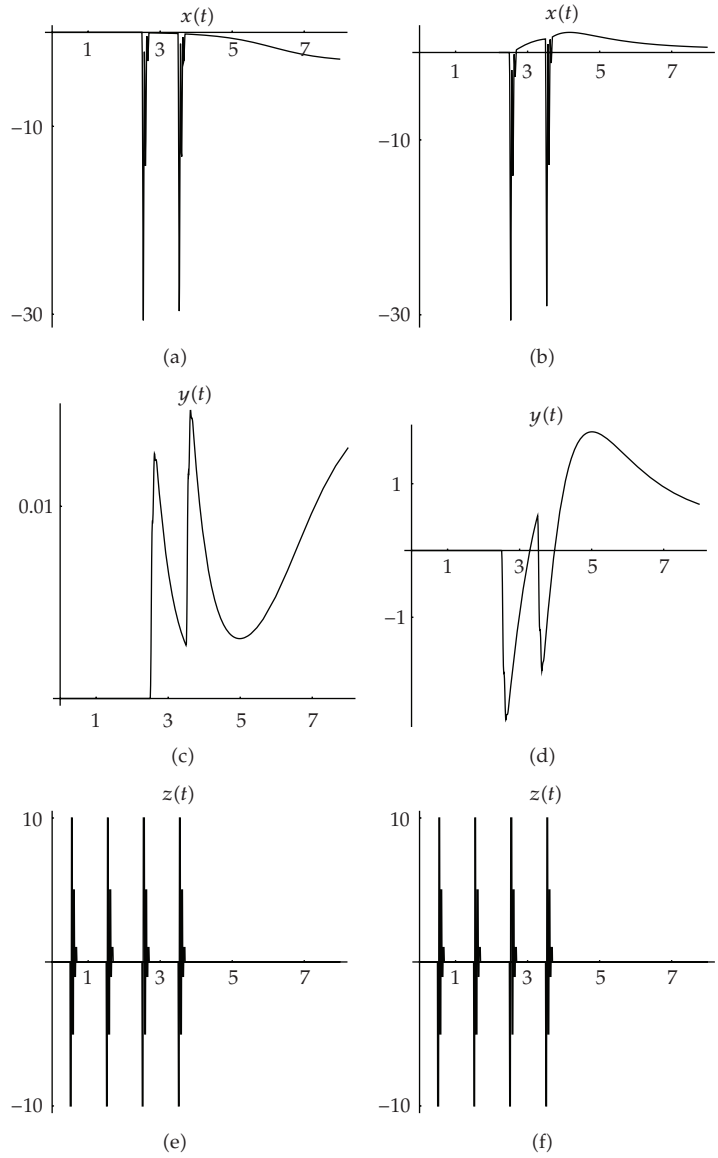

Figure 7: Numerical solution of (3.1) with $\gamma = 10^2$, $\beta = 2$, and $\alpha = -0.01$ (a, c, e), $\alpha = 2$ (b, d, f) in the interval $t \in [0, 8]$; the initial conditions are $x_0 = 0$, $y_0 = 0$.

There follows that, the matrix of the wavelet transform is expressed as a direct sum of lower-order matrices so that the short transform is a sparse matrix [14]. When the short wavelet transform maps short interval values into a few set of wavelet coefficients, it can be considered as a first-order approximation. However, since the wavelet transform maps the original signal into uncorrelated sequences, the short wavelet transform describes, for each sequence of detail coefficients, its local behavior. When $p_s = p = N,\ \sigma = 1$, the above coincides with the ordinary wavelet transform. We assume, in the following, that $p_s = p = N/\sigma,\ s = 0, \ldots, \sigma - 1,\ (\sigma > 1)$.

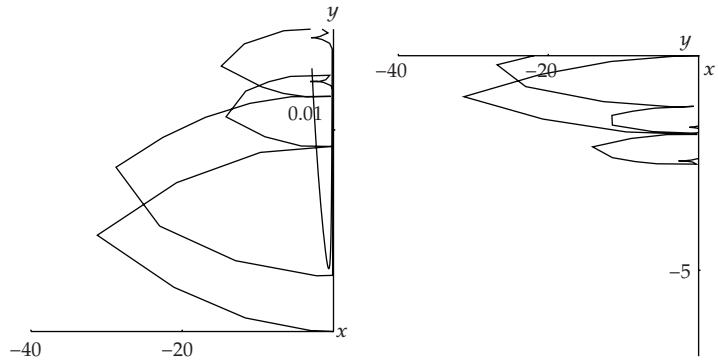

Figure 8: Phase orbits of (3.1) with $\gamma = 10^2$, $\beta = 2$,and $\alpha = -0.01$ (a), $\alpha = 2$ (b) in the interval $t \in [0, 8]$; the initial conditions are $x_0 = 0$, $y_0 = 0$.

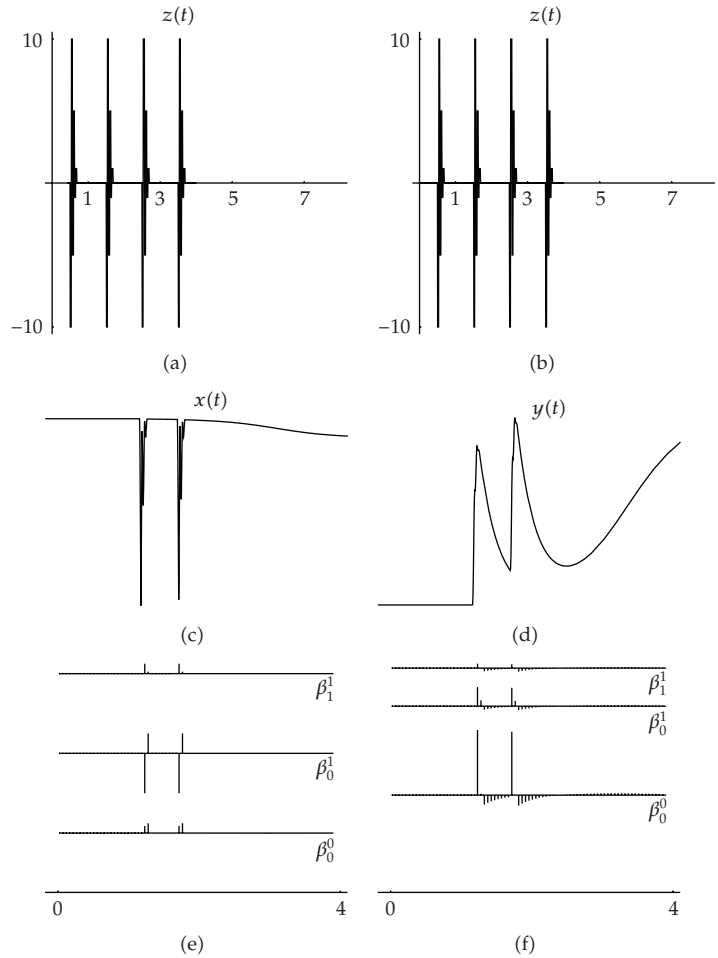

Figure 9: Wavelet coefficients of (3.1) with $\gamma = 10^2$, $\beta = 2$, and $\alpha = -0.01$ in the interval $t \in [0, 8]$; the initial conditions are $x_0 = 0$, $y_0 = 0$.

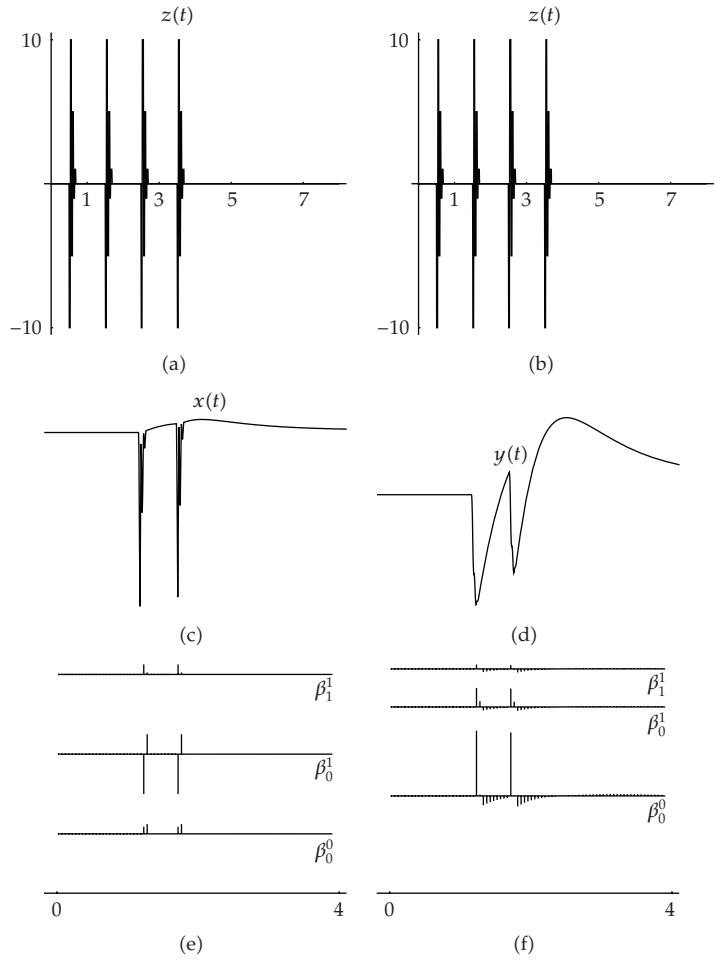

Figure 10: Wavelet coefficients of (3.1) with $\gamma = 10^2$, $\beta = 2$, and $\alpha = 2$ in the interval $t \in [0, 8]$; the initial conditions are $x_0 = 0$, $y_0 = 0$.

4.1. Critical Analysis through the Wavelet Coefficients

Let us take the short Haar wavelet transform for the two time series, obtained by using the Runge-Kutta 4th order method, with the accuracy 10^{-6}, of system (3.1) with the following values of parameters-initial conditions:

$$\gamma = 10^2, \qquad \beta = 2, \qquad x_0 = 0, \qquad y_0 = 0, \qquad t \in [0, 8]. \tag{4.6}$$

The two time series correspond to the two values of α : $\alpha = -0.01$ and $\alpha = 2$. It can be seen from Figures 9 and 10 that the jump is more visible in some coefficients. For instance both in Figure 9 and in Figure 10 the highest value of the amplitude of wavelet coefficients for $x(t)$ is in β_0^1 while for $y(t)$ is in β_0^0. Probably this difference is due to the fact that $x(t)$ is less regular than $y(t)$.

5. Conclusion

In this paper the FitzHugh-Nagumo model has been considered with a high-amplitude pulse. The analysis was done by using wavelet coefficients and it has been shown that the dynamical system shows some kind of inertia against the rapid jumps. In fact, the jumps are detected with some delay with respect to the time they appear.

References

[1] S. El Boustani, M. Pospischil, M. Rudolph-Lilith, and A. Destexhe, "Activated cortical states: experiments, analyses and models," *Journal of Physiology Paris*, vol. 101, no. 1–3, pp. 99–109, 2007.

[2] R. Fitzhugh, "Impulses and physiological states in theoretical models of nerve membrane," *Biophysical Journal*, vol. 1, pp. 455–466, 1961.

[3] N. V. Georgiev, "Identifying generalized Fitzhugh-Nagumo equation from a numerical solution of Hodgkin-Huxley model," *Journal of Applied Mathematics*, no. 8, pp. 397–407, 2003.

[4] J. Guckenheimer and I. S. Labouriau, "Bifurcation of the Hodgkin and Huxley equations: a new twist," *Bulletin of Mathematical Biology*, vol. 55, no. 5, pp. 937–952, 1993.

[5] B. Hassard, "Bifurcation of periodic solutions of the Hodgkin-Huxley model for the squid giant axon," *Journal of Theoretical Biology*, vol. 71, no. 3, pp. 401–420, 1978.

[6] A. L. Hodgkin and A. F. Huxley, "Currents carried by sodium and potassium ions through the membrane of the giant axon of Loligo," *The Journal of Physiology*, vol. 116, pp. 449–472, 1952.

[7] A. L. Hodgkin and A. F. Huxley, "The components of membrane conductance in the giant axon of Loligo," *The Journal of Physiology*, vol. 116, no. 4, pp. 473–496, 1952.

[8] A. L. Hodgkin and A. F. Huxley, "The dual effect of membrane potential on sodium conductance in the giant axon of Loligo," *The Journal of Physiology*, vol. 116, pp. 497–506, 1952.

[9] J. Nagumo, S. Arimoto, and S. Yoshizawa, "An active pulse transmission line simulating nerve axon," *Proceedings of the IRE*, vol. 50, no. 10, pp. 2061–2070, 1962.

[10] J. Rinzel and R. N. Miller, "Numerical calculation of stable and unstable periodic solutions to the Hodgkin-Huxley equations," *Mathematical Biosciences*, vol. 49, no. 1-2, pp. 27–59, 1980.

[11] J. Wang, L. Chen, and X. Fei, "Analysis and control of the bifurcation of Hodgkin-Huxley model," *Chaos, Solitons and Fractals*, vol. 31, no. 1, pp. 247–256, 2007.

[12] G. Mattioli and M. Scalia, "Modelling hodgkin-huxley neurons interaction," in *Proceedings of the International Conference on Computational Science and Its Applications (ICCSA '09)*, vol. 5592 of *Lecture Notes in Computer Science*, pp. 745–751, 2009.

[13] C. Cattani and J. Rushchitsky, *Wavelet and Wave Analysis as Applied to Materials with Micro or Nanostructure*, vol. 74 of *Series on Advances in Mathematics for Applied Sciences*, World Scientific, Hackensack, NJ, USA, 2007.

[14] C. Cattani, "Haar wavelet-based technique for sharp jumps classification," *Mathematical and Computer Modelling*, vol. 39, no. 2-3, pp. 255–278, 2004.